İZMİR KÂTİP ÇELEBİ UNIVERSITY

2010

Body Guidance Synthesis for Sauteing Motion

İslam AYDOĞMUŞ

Abstract

In this project, the goal was to synthesise and analyse a mechanism that can do the same movement as a chef cooks in a frying pan. The main action is based on mixing the daily food put into an average pan in a way that can be thrown up slowly from the end of the pan and lowered back by turning it upside down. Even though compromises had to be made because of the budget limitations, final design supplied the desired motion. The design is based on a four-bar mechanism, provided it can be operated by human power or a small motor. This study utilises kinematic synthesis methodology to generate this mechanism and uses newton's laws to analyse the required minimum torque and bearing reactions to safely operate the mechanism.

Contents

1 Introduction

Kinematic synthesis is the main methodology for any mechanical task to be done with less degrees of freedom. This provides cheaper alternatives for monotonous tasks. For example, simple pick-and-place tasks often over-engineered by using 6 DoF[1] serial robot manipulators. Instead of that, people can use a single DoF mechanism that can be driven by single actuator. This saves running actuator cost, complex engineering calculations thus precious time of the engineer and initial cost to build the system. For these reasons utilising a single degree of freedom system for this sauteing pan motion is very optimised methodology for supplying this motion.

1.1 Body Guidance Synthesis

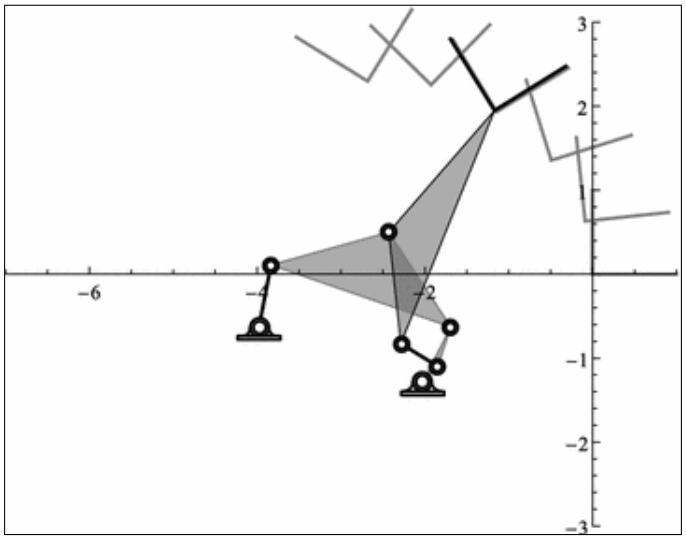

Figure 1.1: *Body Guidance Synthesis* of an arbitrary mechanism. [2]

The methodology intended to be used to generate the mechanism was called *body guidance synthesis* with polynomial approximation. This methodology provides link lengths and constant angles between links for the given precision points so that given mechanism can move through given precision points. These values of links and welding angles are called *construction parameters* of the mechanism. Precision points contains the positions of the desired end-effector and the orientation of the desired link. These values called *variables* of the mechanism.

[1] Degrees of Freedom

1.2 Obtaining Precision Points

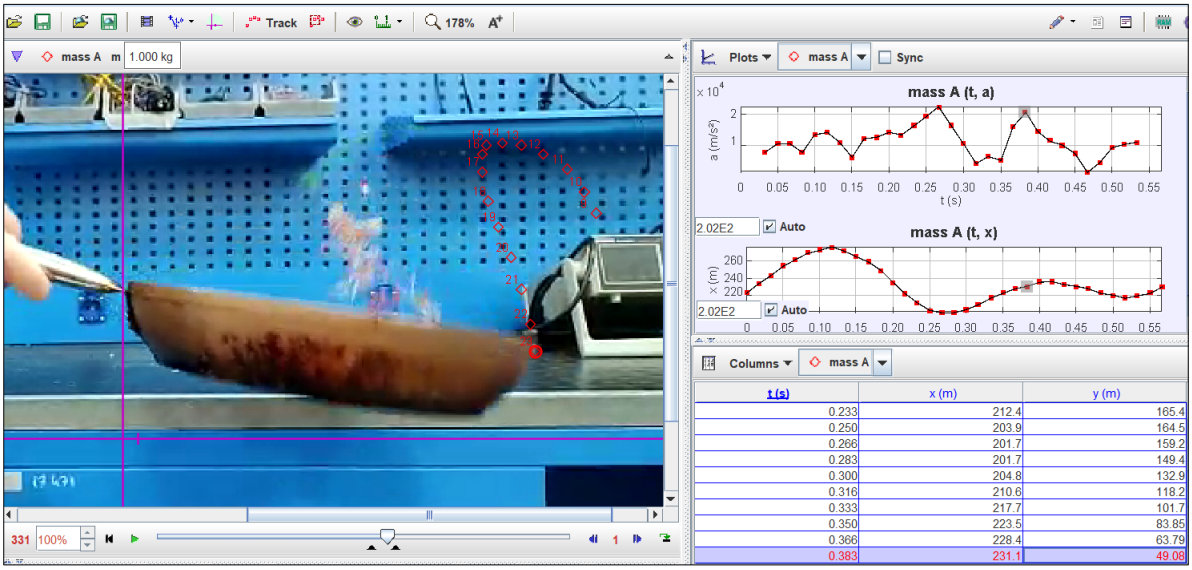

Figure 1.2: Motion capturing process with *Tracker* software. Special thanks to the R.A. Mertcan KOÇAK for helping us capturing this motion.

The desired motion is realised by capturing a handheld video of the movement. Then the motion analysed by a program called *Tracker* and the position and angle data is gathered from the video. The inputs then are fed into the polynomial approximation of our objective function. The results were construction parameters we wanted to obtain. Lastly the mechanism was simulated in the *SolidWorks* CAD software.

2 Kinematic Synthesis

2.1 About Mechanism

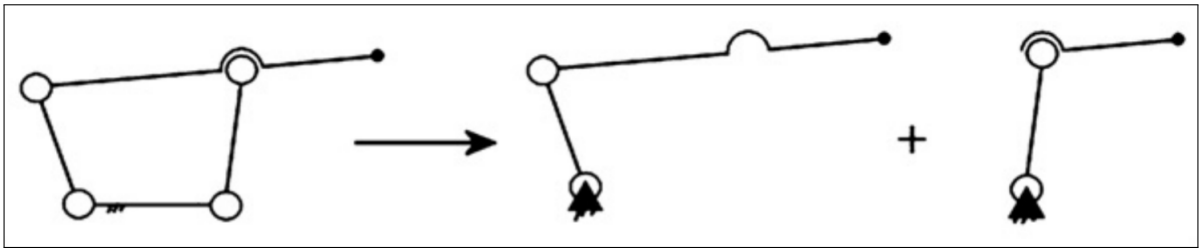

Figure 2.1: Separating four-bar mechanism into two serial manipulators. [1].

The precision points have both coordinates and orientation of the end-effector, namely coupler link, so that analyzed motion can be realised by a simple four bar mechanism. In order to realise the desired four bar, a trick can be made to separate the four-bar into two 2 DoF serial manipulators as can be seen in Figure 2.1.

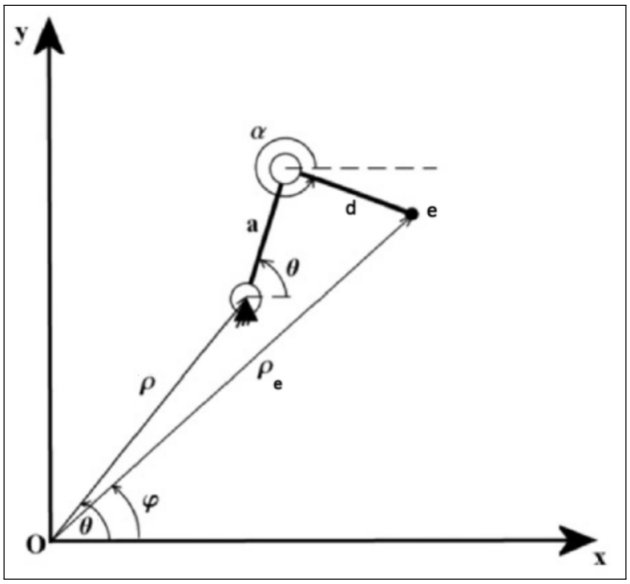

Figure 2.2: Construction parameters and variables of serial manipulator. [1].

construction parameters of $\{a,\ d,\ \rho,\ \theta_1\}$ and *variables* of $\{x_e,\ y_e,\ \theta_1\}$ for serial manipulator are known. Determining construction parameters and variables are important because the method substitutes values to respective variables by *precision points* and tries to obtain construction parameters to, of course, construct the mechanism that will supply the desired motion.

2.2 Obtaining Objective Function

We start obtaining objective function by defining *loop closure equation* for 2 DoF serial manipulator;

$$\vec{\rho} + \vec{a} + \vec{d} = \vec{e} \tag{2.1}$$

... and then separating x and y components of Eqn. (2.1):

$$\rho \cos\theta_1 + a \cos\beta + d \cos\alpha = x_e$$

$$\rho \sin\theta_1 + a \sin\beta + d \sin\alpha = y_e$$

Since we don't want β to be in our objective function, we eliminate it by gathering terms that include β in left-hand side of equation:

$$a \cos\beta = x_e - \rho \cos\theta_1 - d \cos\alpha \tag{2.2}$$

$$a \sin\beta = y_e - \rho \sin\theta_1 - d \sin\alpha \tag{2.3}$$

Now we can eliminate β by squaring both equations (2.2) and (2.3) and summing them:

$$\begin{aligned} a^2(\underbrace{\sin^2\beta + \cos^2\beta}_{=1}) = x_e^2 + y_e^2 + \rho^2(\underbrace{\sin^2\theta_1 + \cos^2\theta_1}_{=1}) + d^2(\underbrace{\sin^2\alpha + \cos^2\alpha}_{=1}) - 2\rho x_e \cos\theta_1 - 2\,d\,x_e \cos\alpha \\ + 2\,\rho\,d\,\cos\alpha\,\cos\theta_1 - 2\,\rho\,y_e\,\sin\theta_1 - 2\,d\,y_e\,\sin\alpha + 2\,\rho\,d\,\sin\alpha\,\sin\theta_1 \end{aligned}$$

Lastly we can reconstruct the equation as:

$$\begin{aligned} 0 = -a^2 + \rho^2 + d^2 + x_e^2 + y_e^2 - 2\,\rho x_e\,\cos\theta_1 - 2\,\rho\,y_e\,\sin\theta_1 + 2\,\rho\,d\,\sin\alpha\,\sin\theta_1 + 2\,\rho\,d\,\cos\alpha\,\cos\theta_1 \\ - 2\,d\,(x_e\,\cos\alpha + y_e\,\sin\alpha) \end{aligned} \tag{2.4}$$

Finally, Eqn. (2.4) is our objective function.

2.3 Polynomial Approximation

Objective polynomial is a specifically arranged version of objective function. Main form we're using are;

$$P_0 f_0 + P_1 f_1 + P_2 f_2 + P_3 f_3 + P_4 f_4 + P_5 f_5 - F = 0 \tag{2.5}$$

... where

$$
\begin{aligned}
P_0 &= \frac{-a^2+\rho^2+d^2}{2\,d}, & f_0 &= 1\\
P_1 &= \frac{1}{d}, & f_1 &= \frac{x_e^2+y_e^2}{2}\\
P_2 &= \rho\,\cos\theta_1, & f_2 &= \cos\alpha\\
P_3 &= \rho\,\sin\theta_1, & f_3 &= \sin\alpha\\
P_4 &= -\frac{\rho\,\cos\theta_1}{d}, & f_4 &= x_e\\
P_5 &= -\frac{\rho\,\sin\theta_1}{d}, & f_5 &= y_e\\
F &= x_e\,\cos\alpha + y_e\,\sin\alpha
\end{aligned}
$$

Note that P_i terms only contains construction parameters while f_i terms only contains variables.

2.4 Non-linear Terms in Polynomial Approximation

Even though we have 6 polynomial constants, we are only allowed to determine 4 precision points since we have only 4 construction parameters. So we have dependent coefficients (or nonlinear parameters) of;

$$
\begin{aligned}
P_4 &= -P_1 P_2\\
P_5 &= -P_1 P_3
\end{aligned}
\tag{2.6}
$$

We're going to address P_4 and P_5 as λ_1 and λ_2 respectively and construct nonlinear equations as:

$$
P_i = l_i + m_i\,\lambda_1 + n_i\,\lambda_2 \tag{2.7}
$$

... for $i = 1, 2, \ldots, 5$.

Now we substitute these parameters into equation (2.5);

$$
\begin{aligned}
(l_0+m_0\,\lambda_1+n_0\,\lambda_2)\,f_0+(l_1+m_1\,\lambda_1+n_1\,\lambda_2)\,f_1+(l_2+m_2\,\lambda_1+n_2\,\lambda_2)\,f_2+(l_3+m_3\,\lambda_1+n_3\,\lambda_2)\,f_3\\
+\lambda_1\,f_4+\lambda_2\,f_5-F=0
\end{aligned}
\tag{2.8}
$$

Now we can separate the equation (2.8) into its three components namely linear, first nonlinear and second nonlinear components;

$$
\begin{aligned}
l_0\,f_0 + l_1\,f_1 + l_2\,f_2 + l_3\,f_3 &= F\\
m_0\,f_0 + m_1\,f_1 + m_2\,f_2 + m_3\,f_3 &= -f_4\\
n_0\,f_0 + n_1\,f_1 + n_2\,f_2 + n_3\,f_3 &= -f_5
\end{aligned}
$$

... and then start to construct respective matrices:

$$\underbrace{\begin{bmatrix} f_0^1 & f_1^1 & f_2^1 & f_3^1 \\ f_0^2 & f_1^2 & f_2^2 & f_3^2 \\ f_0^3 & f_1^3 & f_2^3 & f_3^3 \\ f_0^4 & f_1^4 & f_2^4 & f_3^4 \end{bmatrix}}_{\mathbf{A}} \underbrace{\begin{bmatrix} l_0 \\ l_1 \\ l_2 \\ l_3 \end{bmatrix}}_{\mathbf{L}} = \underbrace{\begin{bmatrix} F^1 \\ F^2 \\ F^3 \\ F^4 \end{bmatrix}}_{\mathbf{F}}$$

$$\mathbf{A} \cdot \underbrace{\begin{bmatrix} m_0 \\ m_1 \\ m_2 \\ m_3 \end{bmatrix}}_{\mathbf{M}} = \underbrace{\begin{bmatrix} -f_4^1 \\ -f_4^2 \\ -f_4^3 \\ -f_4^4 \end{bmatrix}}_{\mathbf{f_4}} \qquad \mathbf{A} \cdot \underbrace{\begin{bmatrix} n_0 \\ n_1 \\ n_2 \\ n_3 \end{bmatrix}}_{\mathbf{N}} = \underbrace{\begin{bmatrix} -f_5^1 \\ -f_5^2 \\ -f_5^3 \\ -f_5^4 \end{bmatrix}}_{\mathbf{f_5}}$$

Where superscript indicates the value of the parameter at the respective precision point. Now we can calculate values of **L**, **M** and **N** by substituting precision points and calculating below equations;

$$\begin{aligned} \mathbf{L} &= \mathbf{A^{-1}} \cdot \mathbf{F} \\ \mathbf{M} &= \mathbf{A^{-1}} \cdot \mathbf{f_4} \\ \mathbf{N} &= \mathbf{A^{-1}} \cdot \mathbf{f_5} \end{aligned}$$

Since we now know matrices **L**, **M** and **N**; we can find λ_1 and λ_2 by solving substituting equations (2.7) into equations (2.6);

$$\begin{aligned} \lambda_1 &= -(l_1 + m_1\,\lambda_1 + n_1\,\lambda_2)\,(l_2 + m_2\,\lambda_1 + n_2\,\lambda_2) \\ \lambda_2 &= -(l_1 + m_1\,\lambda_1 + n_1\,\lambda_2)\,(l_3 + m_3\,\lambda_1 + n_3\,\lambda_2) \end{aligned} \tag{2.9}$$

... so we'll obtain results;

$$\begin{aligned} \lambda_1 &= \{\lambda_{11}, \lambda_{12}, \lambda_{13}\} \\ \lambda_2 &= \{\lambda_{21}, \lambda_{22}, \lambda_{23}\} \end{aligned} \tag{2.10}$$

... since we had third degree polynomial in above equations.

Now we can solve for P_0, P_1, P_2 and P_3 with solutions from Eqns. (2.10). Two of these, reasonable, solutions will give us enough information to find construction parameters of the desired four-bar mechanism that can be seen in Fig. 2.1.

3 Calculations

PP	x_e (cm)	y_e (cm)	α
1	29.96	5.673	-9.1°
2	32.20	7.410	-6.9°
3	33.60	10.14	-3.1°
4	33.46	13.59	2.4°

Table 1: Precision Points used in the synthesis

We substituted precision points indicated into Table 1 in matrices **A**, **F**, $\mathbf{f}_4$ and $\mathbf{f}_5$ and calculated vectors **L**, **M** and **N** by method we've discussed earlier.

$$\begin{bmatrix} l_0 \\ l_1 \\ l_2 \\ l_3 \end{bmatrix} = \begin{bmatrix} 69.3173 \\ 0.0344 \\ -57.6962 \\ -2.2400 \end{bmatrix} \qquad \begin{bmatrix} m_0 \\ m_1 \\ m_2 \\ m_3 \end{bmatrix} = \begin{bmatrix} -39.5363 \\ -0.0367 \\ 29.4086 \\ 15.1446 \end{bmatrix} \qquad \begin{bmatrix} n_0 \\ n_1 \\ n_2 \\ n_3 \end{bmatrix} = \begin{bmatrix} 43.2785 \\ -0.0014 \\ -54.5544 \\ -35.1047 \end{bmatrix} \tag{3.1}$$

Now we can use results of **L**, **M** and **N** in (3.1) on Eqn. (2.9) to find the three pairs of answers on the form of (2.10).

$$\begin{aligned} \lambda_1 &= \{11.1469,\ 0.50908,\ 0.21908\} \\ \lambda_2 &= \{4.41488,\ -0.19867,\ -0.79306\} \end{aligned} \tag{3.2}$$

Finally we can substitute both of the results (3.2) and (3.1) into Eqn. (2.7) to obtain the values of P_0, P_1, P_2 and P_3 (Since we have three λ pairs, we will get three different possible result for each construction parameters).

$$P_0 = \frac{-a^2 + \rho^2 + d^2}{2\,d} = -180.3200 \qquad P_1 = \frac{1}{d} = -0.3809$$
$$P_2 = \rho\,\cos\theta_1 = 29.2666 \qquad P_3 = \rho\,\sin\theta_1 = 11.5914$$

So construction parameters for given set of equations are;

No.	a (cm)	d (cm)	ρ (cm)	θ_1
1	7.14	-2.63	31.48	21.61°
2	3.14	62.64	34.23	158.68°
3	17.59	36.46	30.00	105.44°

Table 2: Construction Parameters of the Mechanism

As we can clearly see, construction parameters that Table 2 no. 1 suggested aren't reasonable since we can't have negative link lengths. However this isn't a problem at all since we only needed two set of logical construction parameters to construct four-bar mechanism that can be seen in the Figure 2.1.

4 Results of Polynomial Synthesis

4.1 General Mechanism

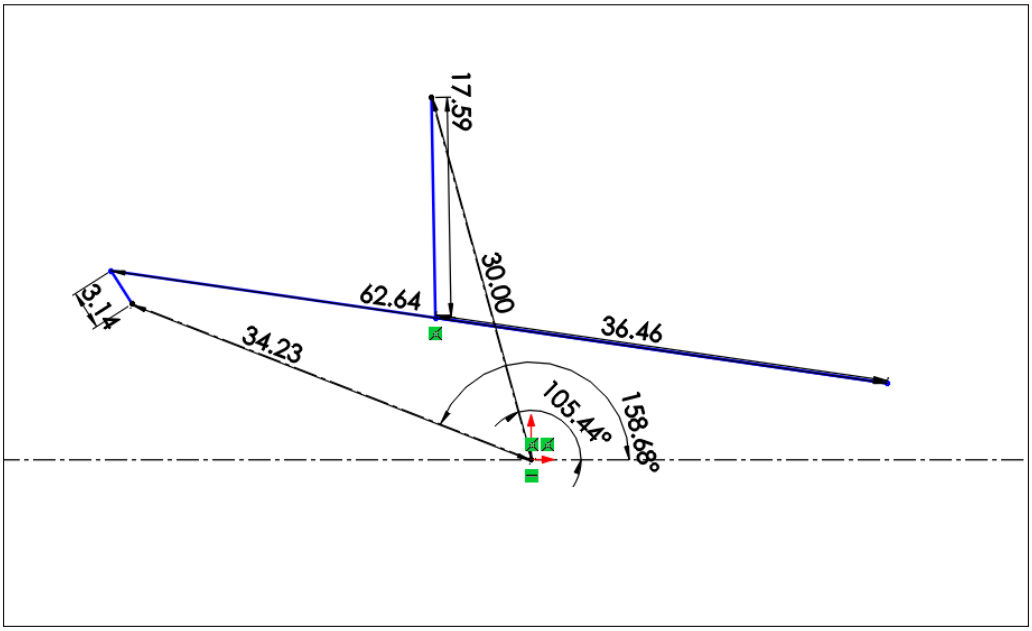

Figure 4.1: Mechanism constructed by construction parameters from Table 2.

Mechanism generated brought a wonderful new perspective about how individual can realise this motion. At the start of this project, the ground links of the result were expected to be closer to a four-bar mechanism like in Figure 2.1, but the mechanism generated uses one of the links to supply the circular motion of frying operation, other link supports the movement by swinging the mechanism like a cradle. This result not seems like important but it is so novel and so simple that, you cannot do much but enjoy.

4.2 Performance at Precision Points

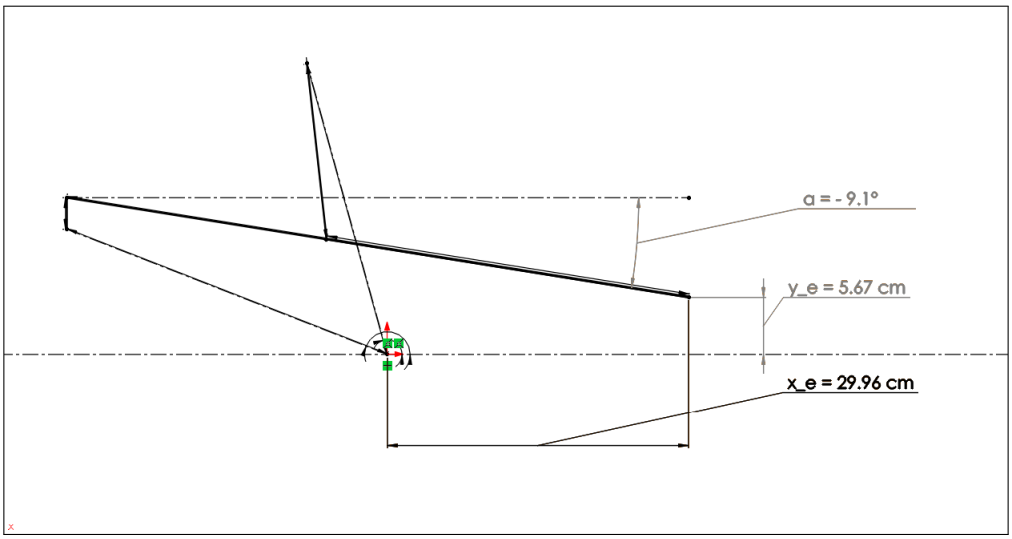

Figure 4.2: Mechanism at first precision Point

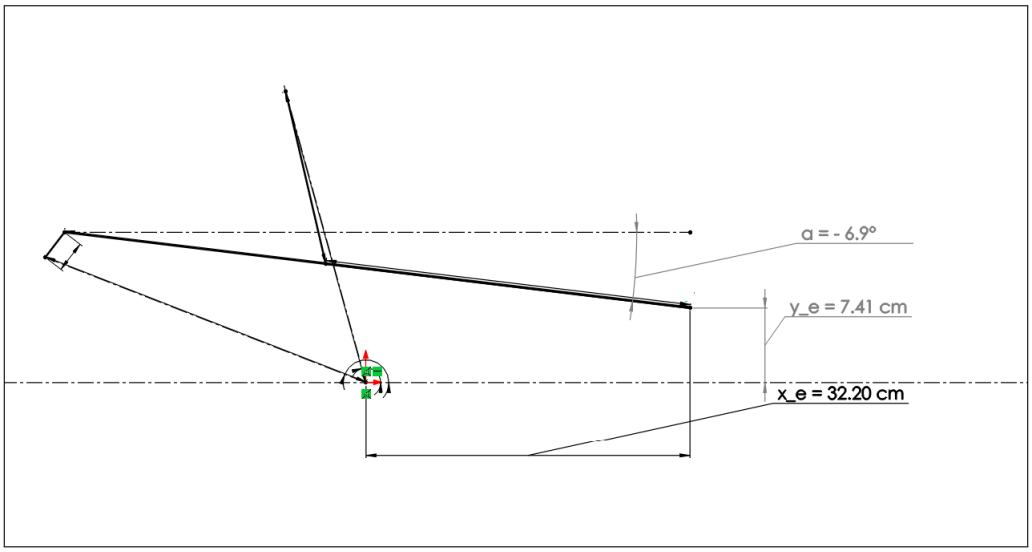

Figure 4.3: Mechanism at second precision Point

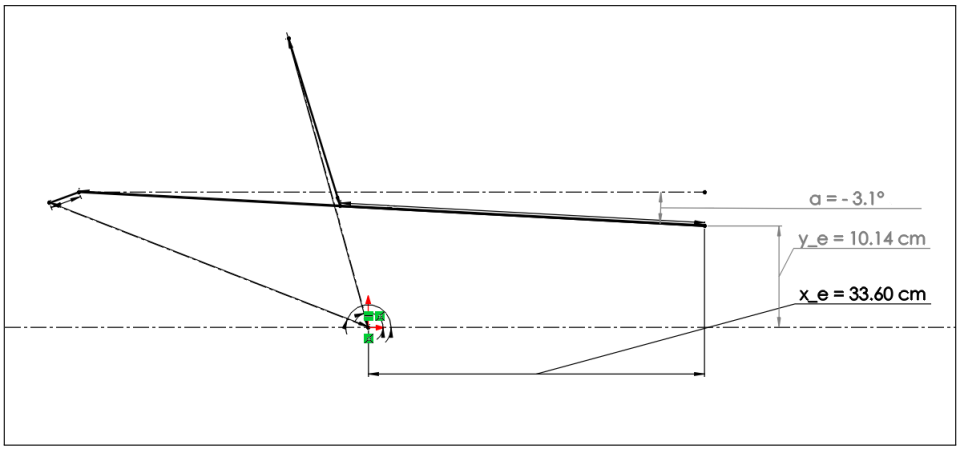

Figure 4.4: Mechanism at third precision Point

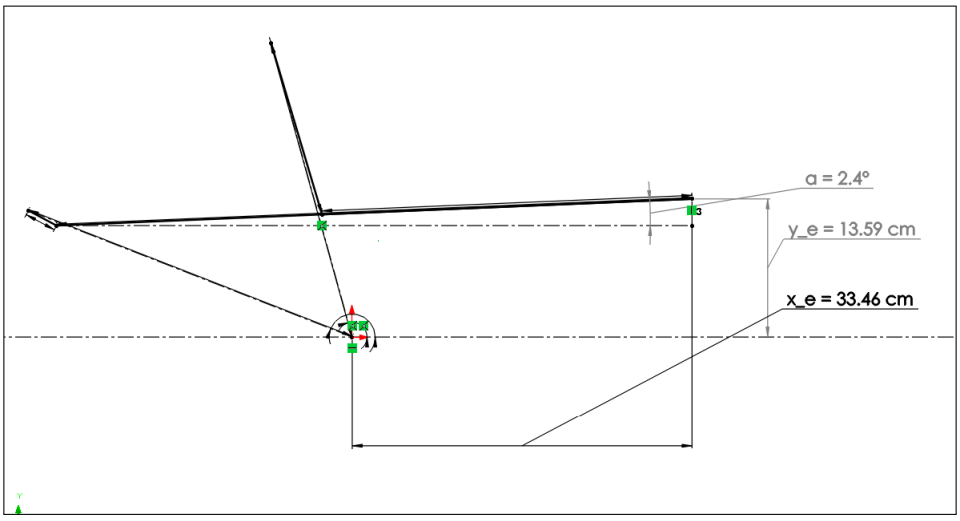

Figure 4.5: Mechanism at fourth precision Point

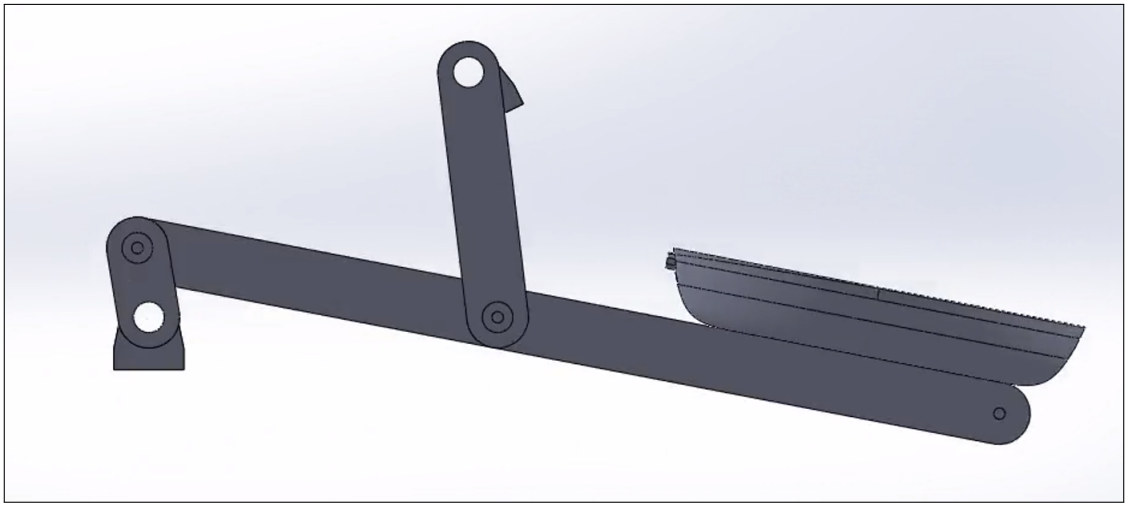

Figure 4.6: A very simple prototype of our results.

5 Final Design

5.1 Scaling the Mechanism

3D printing were used to manufacture the mechanism. As you can see from Table 2 construction parameters of our mechanism weren't suitable for 3D printing. The 3D printer had 220x220x250 printing space in so compromises had to be made.

Firstly the pan changed with a new smaller one. The previous pan that you can see in Fig. 1.2 had 28 cm diameter. New smaller pan has 18 cm diameter. For this reason every construction parameter scaled by 18/28 multiplier. Unfortunately even this scaling weren't enough for limited printing space the 3D printer so the parameters changed until it fits into our limitations. Final construction parameters are:

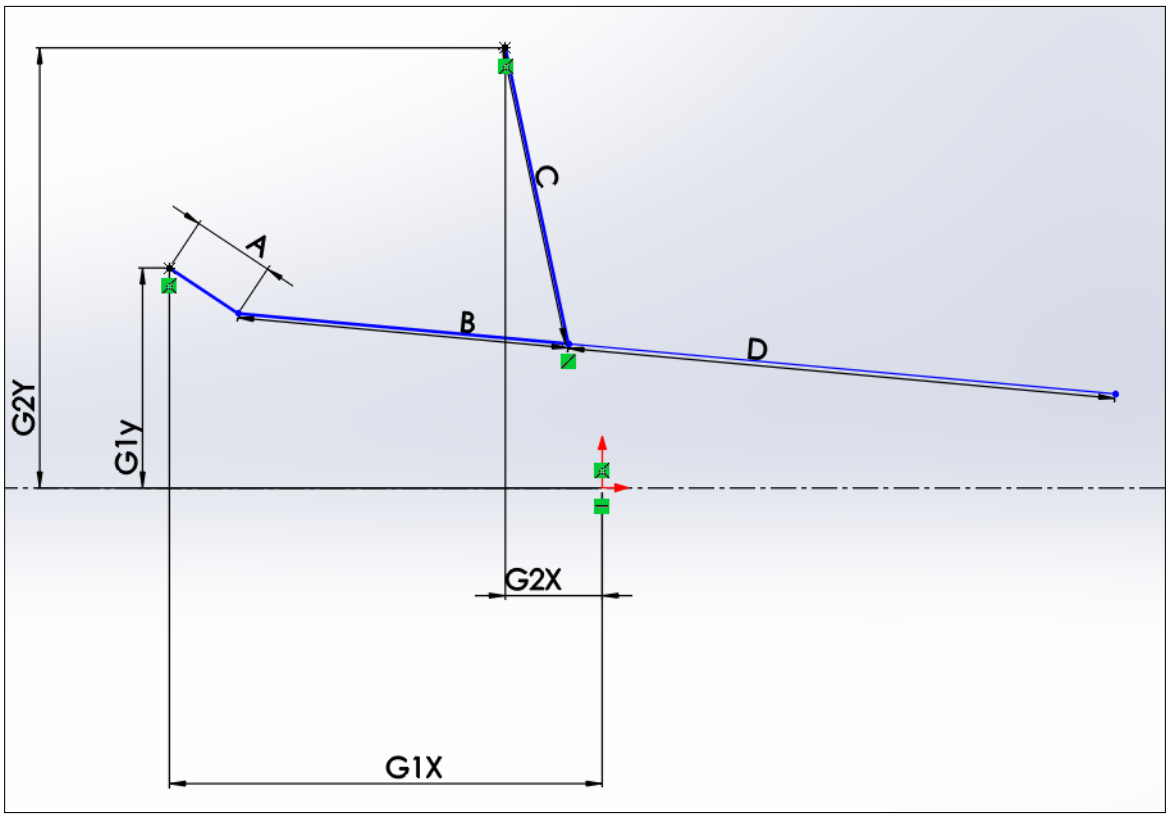

Figure 5.1: Final Construction Parameters

A (cm)	B (cm)	C (cm)	D (cm)	G1x (cm)	G1y (cm)	G2x (cm)	G2y (cm)
3.00	12.81	11.00	20.00	15.76	8.00	3.53	16.00

Table 3: Construction Parameters of the Mechanism that is indicated in Fig. 5.1.

Now the new mechanism look like below figure in SolidWorks:

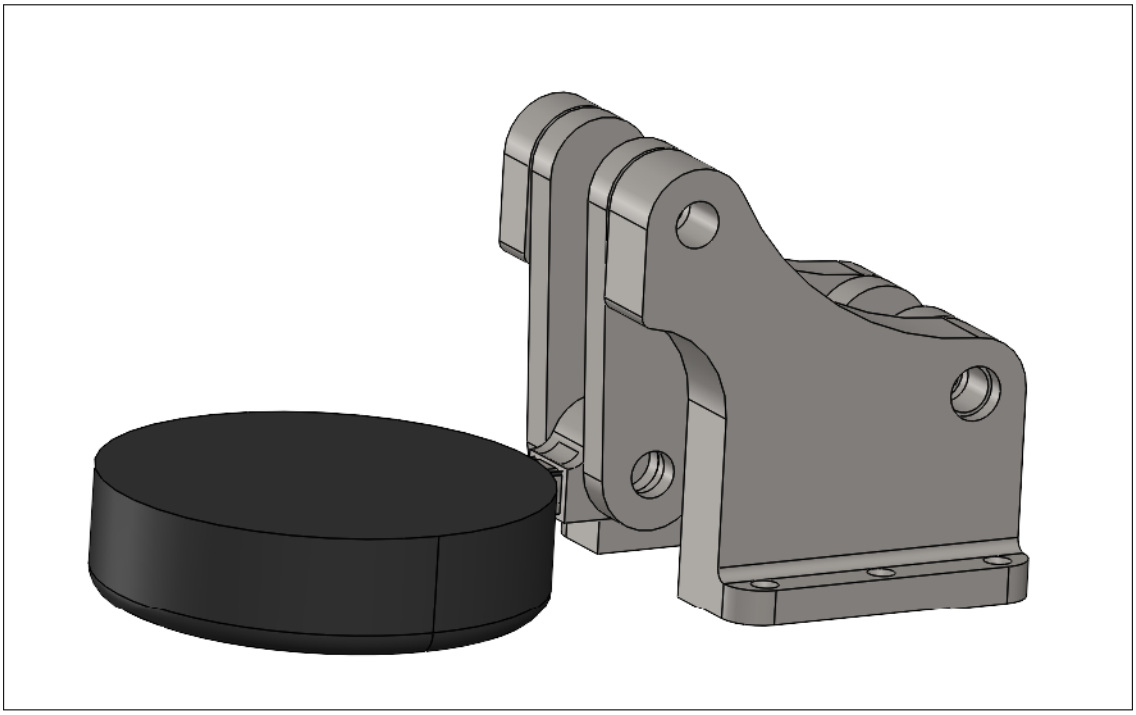

Figure 5.2: Designed mechanism.

6 Kinematic Analysis

6.1 Identifying the tasks

The main task for kinematic analysis is to find the acceleration of crucial points so that it can be used to find find forces acting on the body via Newton's Equations. This allows the required minimum torque for our crank to support the motion desired to be found.

6.2 Obtaining Outputs in Terms of Inputs

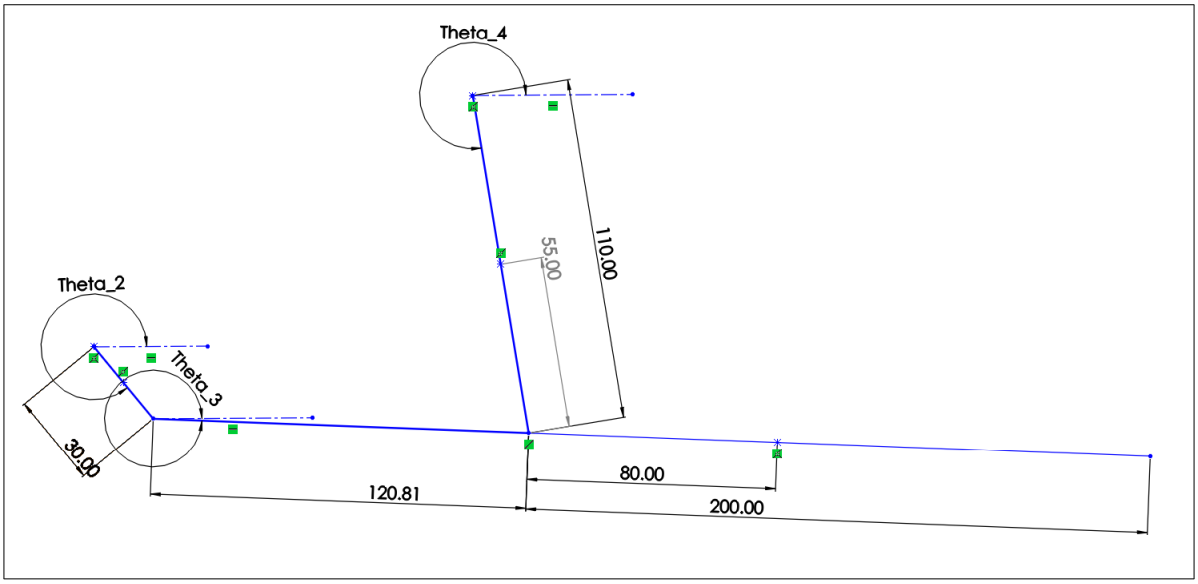

Figure 6.1: We logged θ_3 and θ_4 for given θ_2

Kinematic analysis of the mechanism includes finding θ_3 and θ_4 in terms of θ_2 so that only independent variable of the position equations could be only the input angle. Numeric approach determined to be used to gather the position, velocity and acceleration data for the mechanism. All θ_3 and θ_4 values for given θ_2 values were logged for every 2 degrees in *SolidWorks* Software. Finally we had 180 values each for θ_3 and θ_4 values for given 180 θ_2 values.

The data were logged every 2 degrees. Since period T needed to be found for our numerical derivation progress, the angular velocity that rotating the crank had to be determined. Most likely 60rpm DC motor going to be utilized, so calculations came out as following;

$$\omega[n] = \frac{\theta[n+1] - \theta[n]}{T} \qquad \alpha[n] = \frac{\omega[n+1] - \omega[n]}{T}$$

. . . where

$$T = \frac{1}{180}[sec]$$

6.3 Position Analysis

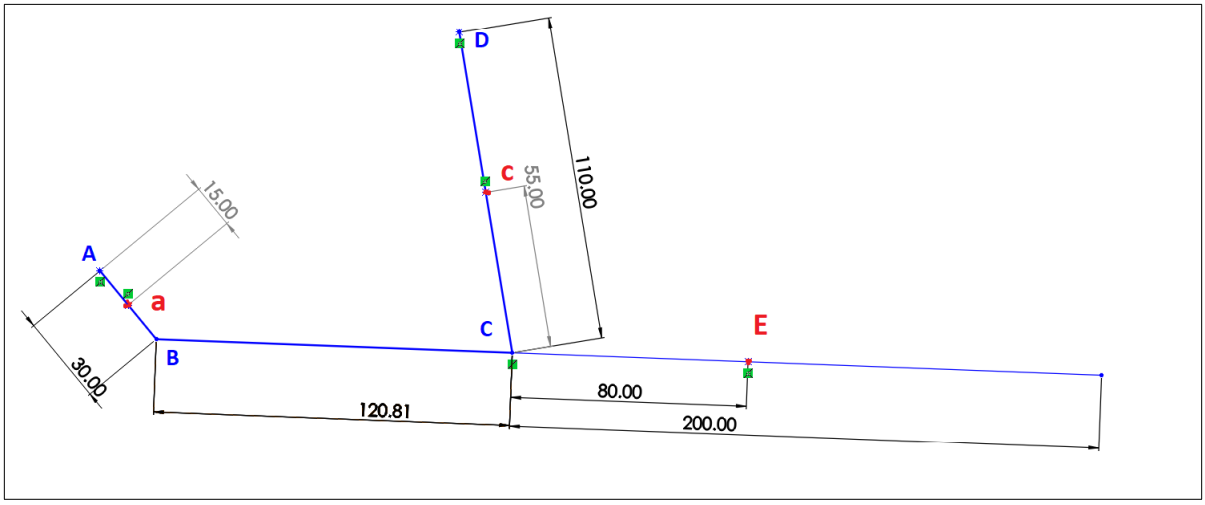

Figure 6.2: Positions of centers of masses of the 3 links (Units are millimeters).

We want to find position vectors of points a, E, and c which is center of mass of l_2, l_3, and l_3 respectively. So given vectors are constructed for these purposes:

$$\begin{aligned}
\boldsymbol{A} &= 0\,\hat{\boldsymbol{\imath}} + 0\,\hat{\boldsymbol{\jmath}} \\
\boldsymbol{a} &= 0.015 \cdot \cos\theta_2\,\hat{\boldsymbol{\imath}} + 0.015 \cdot \sin\theta_2\,\hat{\boldsymbol{\jmath}} \\
\boldsymbol{B} &= 0.03 \cdot \cos\theta_2\,\hat{\boldsymbol{\imath}} + 0.03 \cdot \sin\theta_2\,\hat{\boldsymbol{\jmath}} \\
\boldsymbol{C} &= 0.12081 \cdot \cos\theta_3\,\hat{\boldsymbol{\imath}} + 0.12081 \cdot \sin\theta_3\,\hat{\boldsymbol{\jmath}} + \boldsymbol{B} \\
\boldsymbol{c} &= 0.055 \cdot \cos\theta_4\,\hat{\boldsymbol{\imath}} + 0.055 \cdot \sin\theta_4\,\hat{\boldsymbol{\jmath}} + \boldsymbol{D} \\
\boldsymbol{E} &= 0.20081 \cdot \cos\theta_3\,\hat{\boldsymbol{\imath}} + 0.20081 \cdot \sin\theta_3\,\hat{\boldsymbol{\jmath}} + \boldsymbol{B}
\end{aligned}$$

6.4 Velocity Analysis

We want to find the velocity vectors for a, E, and c, so we're going to differentiate the position vectors in order to obtain velocity vectors:

$$\begin{aligned}
\dot{\boldsymbol{a}} &= -0.015 \cdot \sin\theta_2\,\dot{\theta}_2\,\hat{\boldsymbol{\imath}} + 0.015 \cdot \cos\theta_2\,\dot{\theta}_2\,\hat{\boldsymbol{\jmath}} \\
\dot{\boldsymbol{c}} &= -0.055 \cdot \sin\theta_4\,\dot{\theta}_4\,\hat{\boldsymbol{\imath}} + 0.055 \cdot \cos\theta_4\,\dot{\theta}_4\,\hat{\boldsymbol{\jmath}} \\
\dot{\boldsymbol{E}} &= (-0.06\,\sin\theta_2\,\dot{\theta}_2 - 0.32162\,\sin\theta_3\,\dot{\theta}_3)\,\hat{\boldsymbol{\imath}} + (0.06\,\cos\theta_2\,\dot{\theta}_2 + 0.32162\,\cos\theta_3\,\dot{\theta}_3)\,\hat{\boldsymbol{\jmath}}
\end{aligned}$$

6.5 Acceleration Analysis

Finally we want to obtain the acceleration vectors for a, E, and c, so we're going to differentiate the velocity vectors in order to obtain velocity vectors:

$$\ddot{\boldsymbol{a}} = (-0.015 \sin(\theta_2(t)) \frac{\partial^2}{\partial t^2} \theta_2(t) - 0.015 \cos(\theta_2(t)) \left(\frac{\partial}{\partial t} \theta_2(t)\right)^2) \hat{\boldsymbol{\imath}} + (0.015 \cos(\theta_2(t)) \frac{\partial^2}{\partial t^2} \theta_2(t) - 0.015 \sin(\theta_2(t)) \left(\frac{\partial}{\partial t} \theta_2(t)\right)^2) \hat{\boldsymbol{\jmath}}$$

$$\ddot{\boldsymbol{c}} = (-0.055 \sin(\theta_4(t)) \frac{\partial^2}{\partial t^2} \theta_4(t) - 0.055 \cos(\theta_4(t)) \left(\frac{\partial}{\partial t} \theta_4(t)\right)^2) \hat{\boldsymbol{\imath}} + (0.055 \cos(\theta_4(t)) \frac{\partial^2}{\partial t^2} \theta_4(t) - 0.055 \sin(\theta_4(t)) \left(\frac{\partial}{\partial t} \theta_4(t)\right)^2) \hat{\boldsymbol{\jmath}}$$

$$\ddot{\boldsymbol{E}} = (-0.06 \cos(\theta_2(t)) \sigma_2 - 0.32162 \cos(\theta_3(t)) \sigma_1 - 0.06 \sin(\theta_2(t)) \sigma_4 - 0.32162 \sin(\theta_3(t)) \sigma_3) \hat{\boldsymbol{\imath}} + (0.06 \cos(\theta_2(t)) \sigma_4 - 0.32162 \sin(\theta_3(t)) \sigma_1 - 0.06 \sin(\theta_2(t)) \sigma_2 + 0.32162 \cos(\theta_3(t)) \sigma_3) \hat{\boldsymbol{\jmath}}$$

... where

$\sigma_1 = \left(\frac{\partial}{\partial t} \theta_3(t)\right)^2$

$\sigma_2 = \left(\frac{\partial}{\partial t} \theta_2(t)\right)^2$

$\sigma_3 = \frac{\partial^2}{\partial t^2} \theta_3(t)$

$\sigma_4 = \frac{\partial^2}{\partial t^2} \theta_2(t)$

6.6 Results

180 position values were differentiated numerically two times and logged. As one can see from Fig. 6.3a and Fig. 6.3b the α(angular acceleration) data were to noisy. To fix this, a discrete low-pass filter were applied to angular acceleration data and those values are used for further calculations. Raw data can be inspected below:

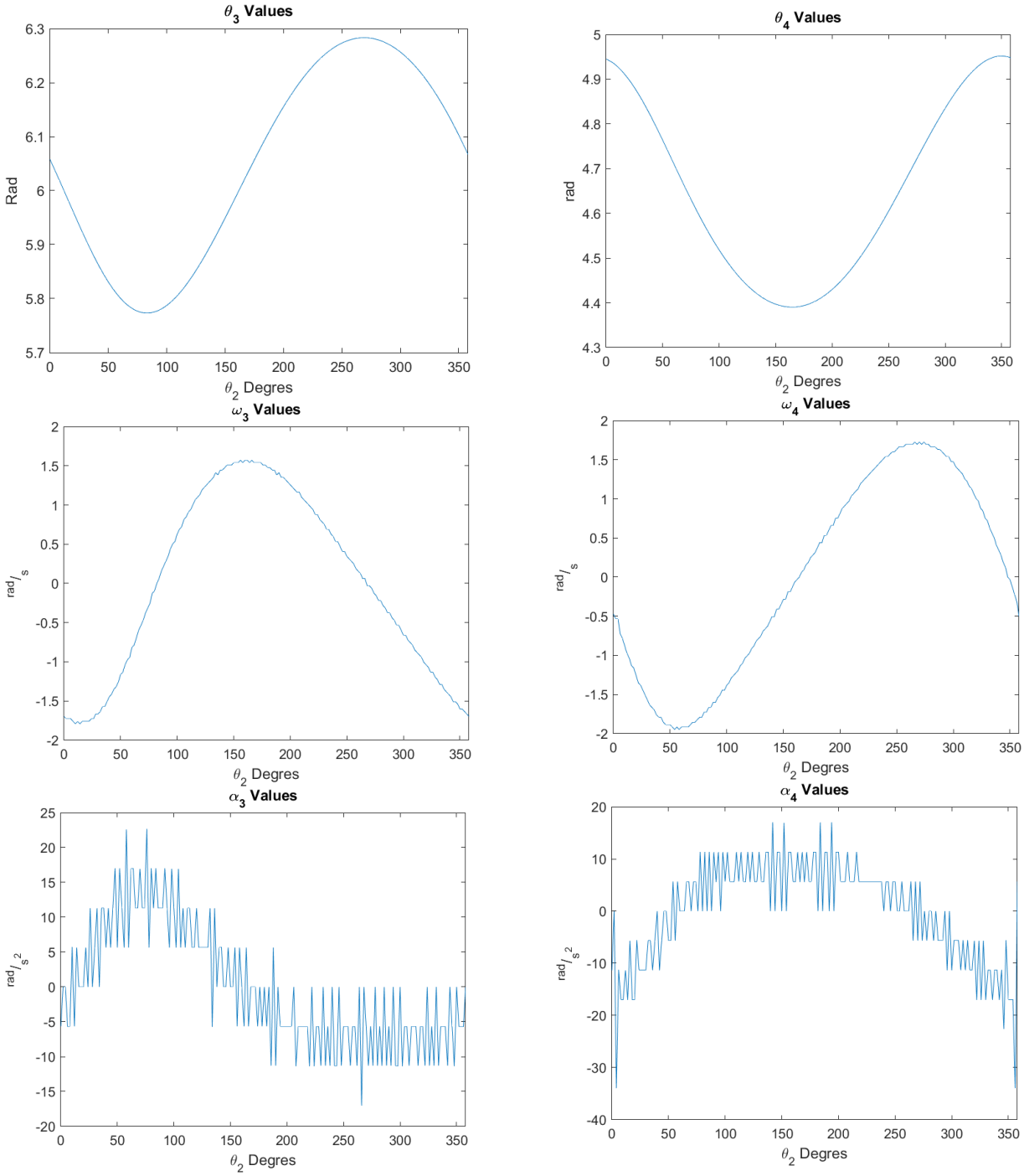

(a) Numerical derivation of ω_3 and α_3 from θ_3. **(b)** Numerical derivation of ω_4 and α_4 from θ_4.

Figure 6.3: Results of kinematic analysis

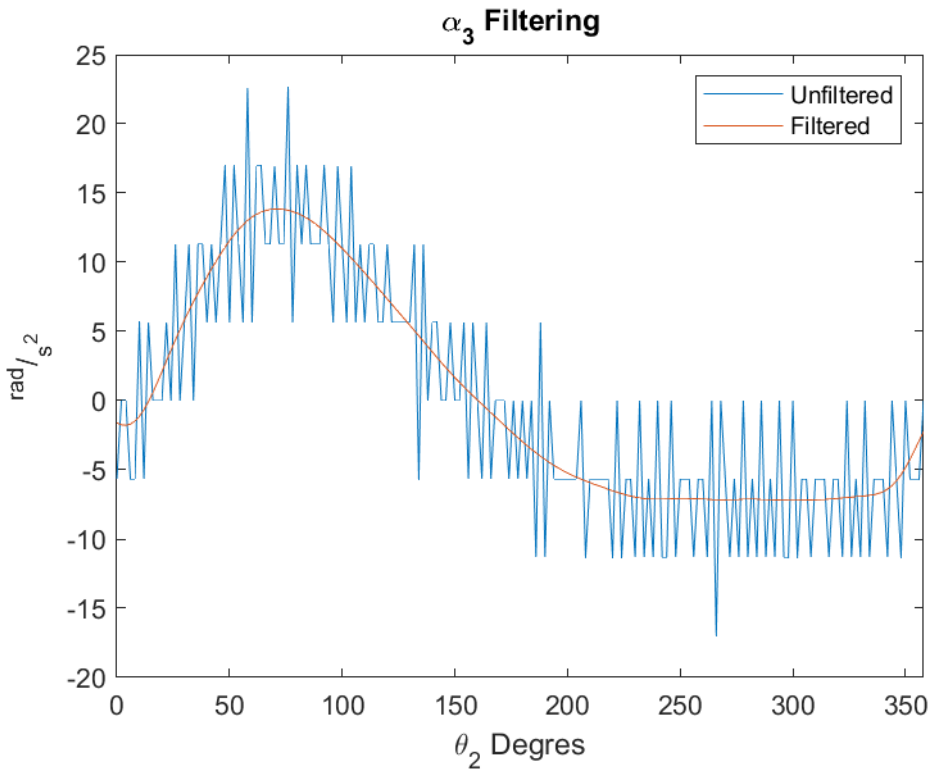

Figure 6.4: Low-pass filtered version of α_3.

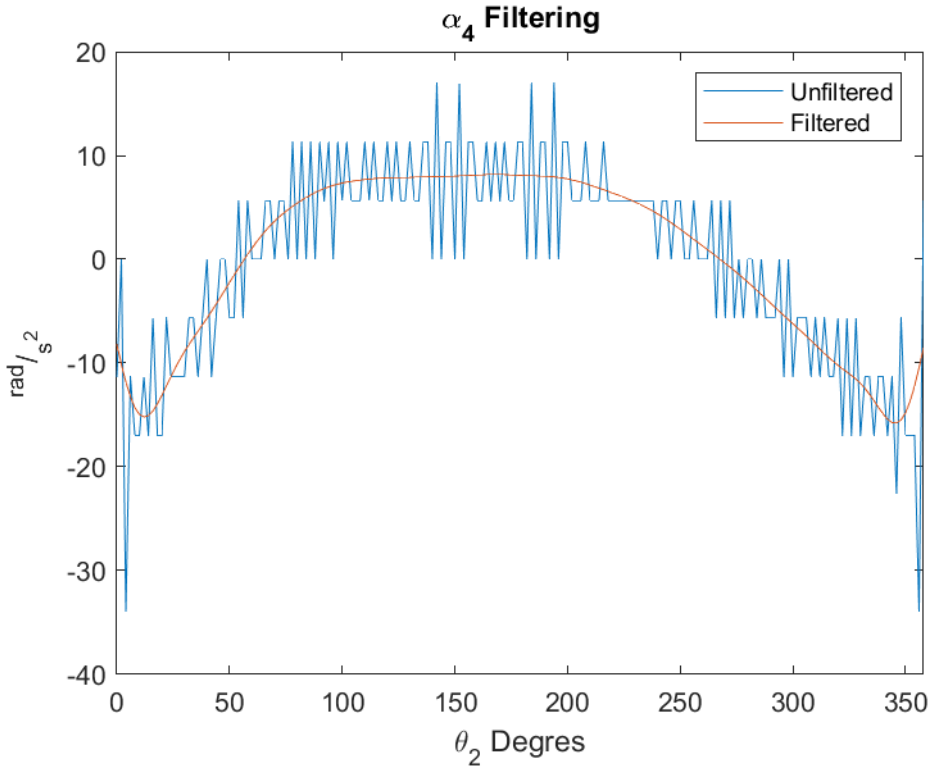

Figure 6.5: Low-pass filtered version of α_4.

7 Dynamic Force Analysis

7.1 Identifying Task

Accelerations of crucial points were found in Kinematic Analysis section. Now with this knowledge, force equations can be constructed. Chosen critical points and their properties can be seen in figure 4. Moment of inertia values are calculated in the section 7.2.

Properties	l_2	l_3	l_4
Mass center(mm)	15.00	200.81	55.00
Mass (grams)	30	1500	80
Moment of inertia (kg·m)	25.8e-6	6.1e-3	0.4e-3

Table 4: Properties.

7.2 Finding Moments of Inertia

All of the links were assumed to be rectangles and following formulas were used for finding the moment of inertia with respect to gravitational centers of the respective links.

$$I_z = \frac{1}{12} m \cdot (h^2 + w^2) \tag{7.1}$$

. . . where
m = Mass [kg]
h = Planar height of the rectangle [m]
w = Planar width of the rectangle [m]

Then *Parallel Axis Theorem* can be used to find the moment of inertia with respect to center of rotation.

$$I = I_c + m \cdot d^2 \tag{7.2}$$

. . . where
I = Moment of inertia of the body $[kg \cdot m^2]$
I_c = Moment of inertia about the center $[kg \cdot m^2]$
d = Distance between the two axes [m]

7.2.1 Crank Link

Sizes of the crank link are 75x45 mm. So respective values become;

Properties	Value
m (kg)	0.030
h (m)	0.075
w (m)	0.045
d (m)	0.015

Table 5: Crank variables.

... moment of inertia of one crank link becomes $25.88 \times 10^{-6}\ kg \cdot m^2$. Since the mechanism has 2 cranks in each side, result can be multiplied by 2 and use that value instead.

7.2.2 Coupler Link (Pan)

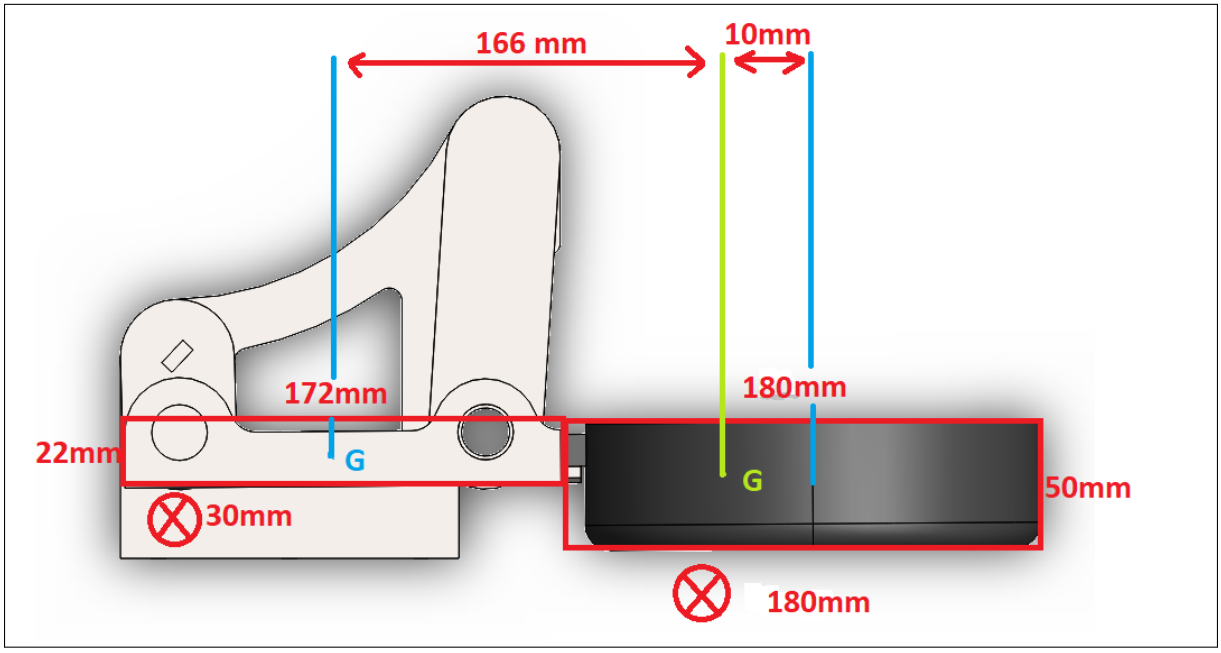

Figure 7.1: Coupler parameters visualised.

The values that is going to be used for the calculations can be seen in Fig. 7.1. These values substituted into equations 7.2 and 7.2. Value of $6.1 \times 10^{-3}\ kg \cdot m^2$ is obtained.

7.2.3 Rocker Link

Sizes of the rocker link are 155x45 mm. So respective values become;

Properties	Value
m (kg)	0.080
h (m)	0.155
w (m)	0.045
d (m)	0.055

Table 6: Rocker variables.

... moment of inertia of one crank link becomes $0.404 \times 10^{-3}\ kg \cdot m^2$. Since the mechanism has 2 rockers in each side, result can be multiplied by 2 and use that value instead.

7.3 Free Body Diagrams

Free body diagrams of each link in the mechanism will construct appropriate relations, and supply the required equations in order to find the unknowns. Mechanism can be inspected at Fig. 6.2.

7.3.1 Crank Link

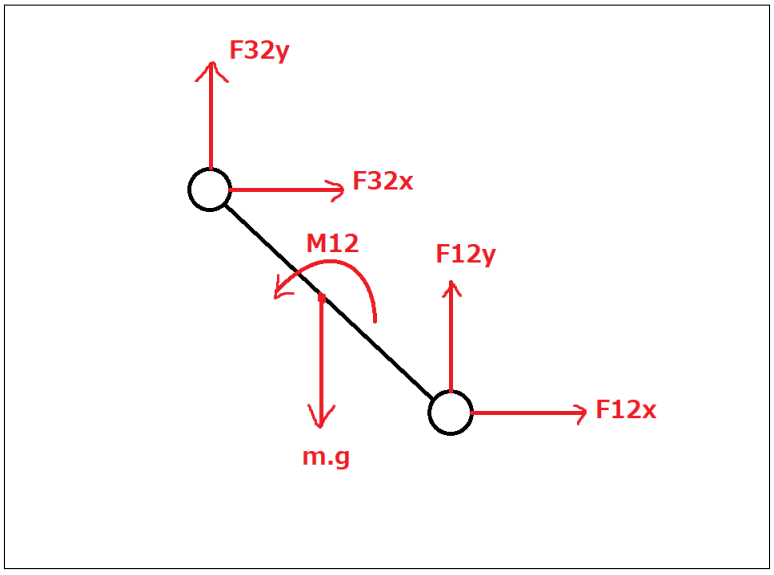

Figure 7.2: FBD of crank link.

This link yields these equations:

$$F_{12,x} + F_{32,x} = m_2\, A_{G_2,x} \tag{7.3}$$

$$-m_2\,g + F_{12,y} + F_{32,y} = m_2\,A_{G_2,y} \tag{7.4}$$

$$0.015\,(-cos\theta_2\,\hat{\boldsymbol{\imath}} - sin\theta_2\,\hat{\boldsymbol{\jmath}}) \times (F_{12,x}\,\hat{\boldsymbol{\imath}} + F_{12,y}\,\hat{\boldsymbol{\jmath}}) + 0.015\,(cos\theta_2\,\hat{\boldsymbol{\imath}} + sin\theta_2\,\hat{\boldsymbol{\jmath}}) \times (F_{32,x}\,\hat{\boldsymbol{\imath}} + F_{32,y}\,\hat{\boldsymbol{\jmath}}) + M_{12} = I_2\,\alpha_2 \tag{7.5}$$

Or equivalently:

$$-0.015\,F_{12,y}\,cos\theta_2 + 0.015\,F_{12,x}\,sin\theta_2 + 0.015\,F_{32,y}\,cos\theta_2 - 0.015\,F_{32,x}\,sin\theta_2 + M_12 = I_2\,\alpha_2 \tag{7.6}$$

7.3.2 Coupler Link

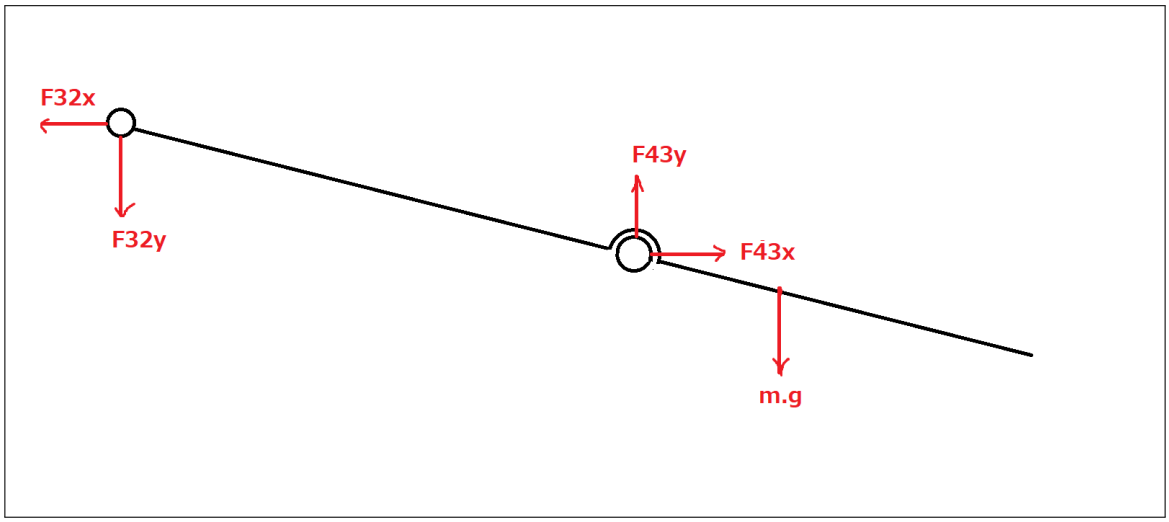

Figure 7.3: FBD of coupler link.

This link yields these equations:

$$-F_{32,x} + F_{43,x} = m_3\,A_{G_3,x} \tag{7.7}$$

$$-m_3\,g - F_{32,y} + F_{43,y} = m_3\,A_{G_3,y} \tag{7.8}$$

$$0.08\,(-cos\theta_3\,\hat{\boldsymbol{\imath}} - sin\theta_3\,\hat{\boldsymbol{\jmath}}) \times (F_{43,x}\,\hat{\boldsymbol{\imath}} + F_{43,y}\,\hat{\boldsymbol{\jmath}}) + 0.20081\,(-cos\theta_3\,\hat{\boldsymbol{\imath}} - sin\theta_3\,\hat{\boldsymbol{\jmath}}) \times (-F_{32,x}\,\hat{\boldsymbol{\imath}} - F_{32,y}\,\hat{\boldsymbol{\jmath}}) = I_3\,\alpha_3 \tag{7.9}$$

Or equivalently:

$$-0.08\,F_{43,y}\,cos\theta_3 + 0.08\,F_{43,x}\,sin\theta_3 + 0.20081\,F_{32,y}\,cos\theta_3 - 0.20081\,F_{32,x}\,sin\theta_3 = I_3\,\alpha_3 \tag{7.10}$$

7.3.3 Rocker Link

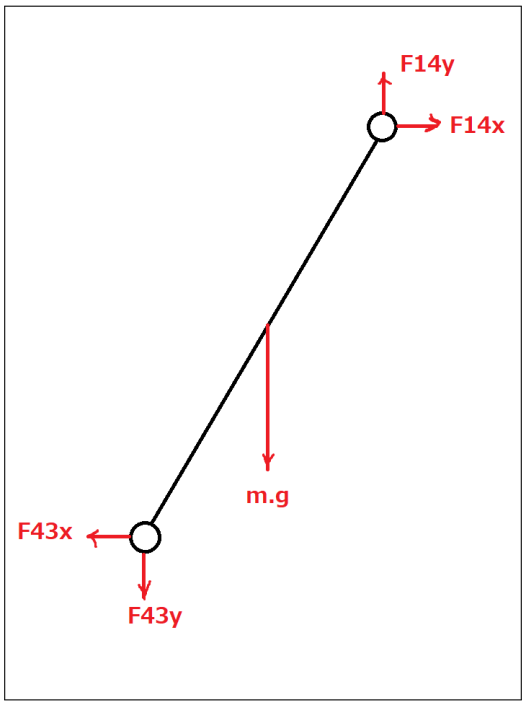

Figure 7.4: FBD of rocker link.

This link yields these equations:

$$-F_{43,x} + F_{14,x} = m_4\, A_{G_4,x} \tag{7.11}$$

$$-m_4\, g - F_{43,y} + F_{14,y} = m_4\, A_{G_4,y} \tag{7.12}$$

$$\begin{aligned} 0.055\,(-cos\theta_4\,\hat{\boldsymbol{\imath}} - sin\theta_4\,\hat{\boldsymbol{\jmath}}) \times (F_{14,x}\,\hat{\boldsymbol{\imath}} + F_{14,y}\,\hat{\boldsymbol{\jmath}}) \\ + 0.055\,(cos\theta_4\,\hat{\boldsymbol{\imath}} + sin\theta_4\,\hat{\boldsymbol{\jmath}}) \times (-F_{43,x}\,\hat{\boldsymbol{\imath}} - F_{43,y}\,\hat{\boldsymbol{\jmath}}) = I_4\,\alpha_4 \end{aligned} \tag{7.13}$$

Or equivalently:

$$-0.055\,F_{14,y}\,cos\theta_4 + 0.055\,F_{14,x}\,sin\theta_4 - 0.055\,F_{43,y}\,cos\theta_4 + 0.055\,F_{43,x}\,sin\theta_4 = I_4\,\alpha_4 \tag{7.14}$$

8 Calculations

Since relatively high number of instances will be calculated (180 values), a coefficient matrix can be derived instead of using classical solve commands to speed up the calculating process. From 9 equations we derived from free body diagrams, we can derive following equation:

$$\begin{pmatrix} 1 & 0 & 1 & 0 & 0 & 0 & 0 & 0 & 0 \\ 0 & 1 & 0 & 1 & 0 & 0 & 0 & 0 & 0 \\ \sigma_3 & -\sigma_4 & -\sigma_3 & \sigma_4 & 0 & 0 & 0 & 0 & 1 \\ 0 & 0 & -1 & 0 & 1 & 0 & 0 & 0 & 0 \\ 0 & 0 & 0 & -1 & 0 & 1 & 0 & 0 & 0 \\ 0 & 0 & -\frac{20081\,\sin(\theta_3)}{100000} & \frac{20081\,\cos(\theta_3)}{100000} & \frac{2\,\sin(\theta_3)}{25} & -\frac{2\,\cos(\theta_3)}{25} & 0 & 0 & 0 \\ 0 & 0 & 0 & 0 & -1 & 0 & 1 & 0 & 0 \\ 0 & 0 & 0 & 0 & 0 & -1 & 0 & 1 & 0 \\ 0 & 0 & 0 & 0 & \sigma_2 & \sigma_1 & \sigma_2 & \sigma_1 & 0 \end{pmatrix} \cdot \begin{pmatrix} F_{12,x} \\ F_{12,y} \\ F_{32,x} \\ F_{32,y} \\ F_{43,x} \\ F_{43,y} \\ F_{14,x} \\ F_{14,y} \\ M_{12} \end{pmatrix}$$

$$= \begin{pmatrix} m_2\,A_{G2,y} \\ m_2\,A_{G2,y} + m_2\,g \\ I_2\,\alpha_2 \\ m_3\,A_{G3,y} \\ m_3\,A_{G3,y} + m_3\,g \\ I_3\,\alpha_3 \\ m_2\,A_{G4,y} \\ m_4\,A_{G4,y} + m_4\,g \\ I_4\,\alpha_4 \end{pmatrix} \tag{8.1}$$

where

$\sigma_1 = -0.055\,\cos(\theta_4)$

$\sigma_2 = 0.055\,\sin(\theta_4)$

$\sigma_3 = 0.055\,\sin(\theta_2)$

$\sigma_4 = 0.055\,\cos(\theta_2)$

With Eqn. (8), values for each of the variable can be found.
Let's revise what the variables were representing. $F_{12,x}$ and $F_{12,y}$ is components of bearing response at crank link, namely A joint in Fig. 6.2. $F_{32,x}$ and $F_{32,y}$ is components of bearing response at joint B on coupler link. $F_{43,x}$ and $F_{43,y}$ is components of bearing response at joint C on coupler link. $F_{14,x}$ and $F_{14,y}$ is components of bearing response at joint D on rocker link, And last but certainly not the least, the M_{12} is the minimum torque we need to supply to rotate the mechanism at 60 RPM. With this knowledge the results can be analysed better.

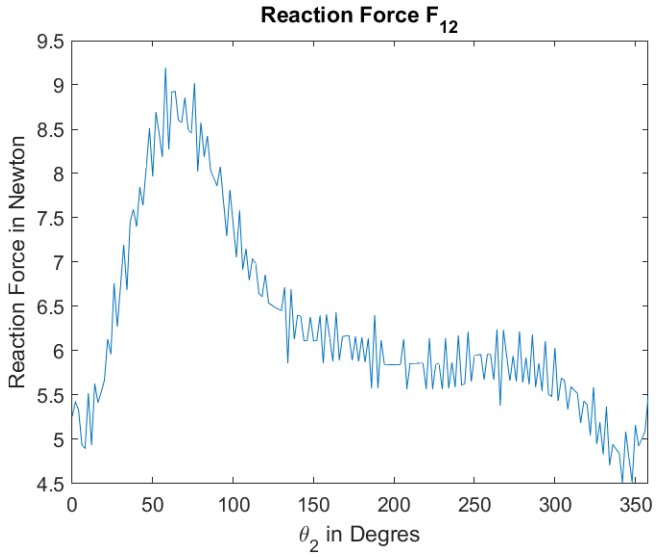

Figure 8.1: Magnitude of F_{12}.

Since the mechanism had 2 bearings that forms joint A in our design, max value can be divided with two to find required minimum bearing radial strength. Which is approximately 10 divided by 2 equals to 5.

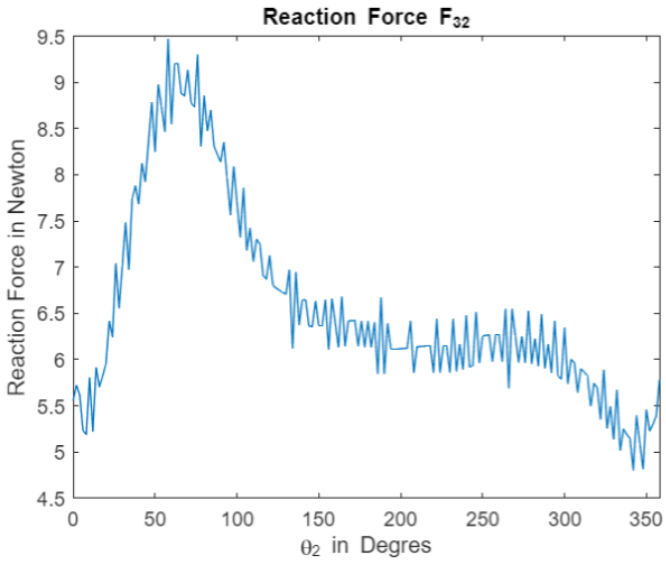

Figure 8.2: Magnitude of F_{32}.

Since the mechanism had 2 bearings that forms joint B in our design, max value can be divided with two to find required minimum bearing radial strength. Which is approximately 10 divided by 2 equals to 5 Newton. Note that F_{12} and F_{32} seems very close to each other. This is because they construct the couple force that builds M_{12} so it's reasonable them to be equal.

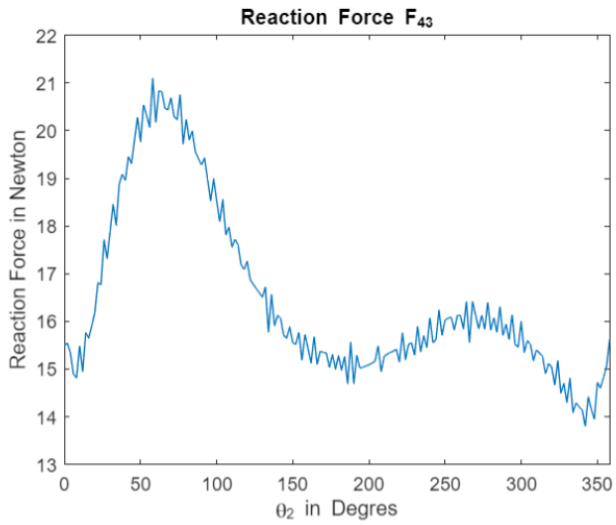

Figure 8.3: Magnitude of F_{43}.

Since the mechanism had 2 bearings that forms joint C in our design, max value can be divided with two to find required minimum bearing radial strength. Which is approximately 22 divided by 2 equals to 11 Newton.

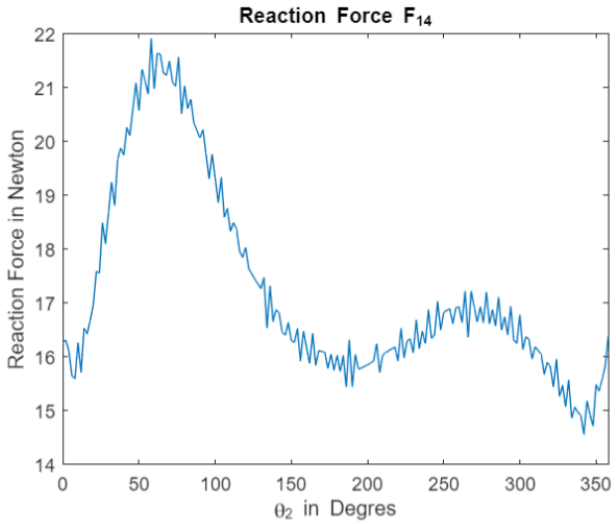

Figure 8.4: Magnitude of F_{14}.

Since the mechanism had 2 bearings that forms joint D in our design, max value can be divided with two to find required minimum bearing radial strength. Which is approximately 22 divided by 2 equals to 11 Newton. Note that F_{43} and F_{13} seems very close to each other. This is because they construct the two force element of link 4 so it's reasonable them to be equal again.

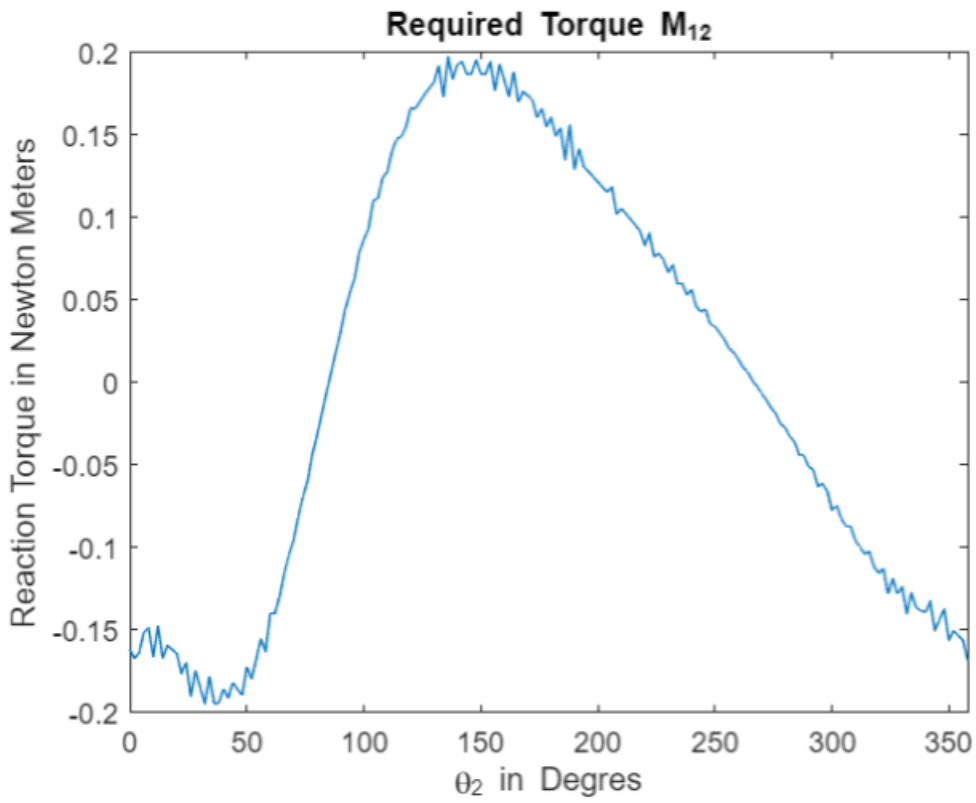

Figure 8.5: Magnitude of M_{12}.

Finally the most important value. As one can see from the figure 8.5, 0.2 N.m torque minimum can supply this movement. This actually approximately equals to 20 N.cm torque which most of the hobby servos can supply.

9 Manufacturing

9.1 Printing the Parts

The first thing we did during the production phase was to make the designed parts removable from the 3D printer. The parts were optimized considering the asymmetries in the parts and the printing technique of the printer. The fill rate of the parts was adjusted to be 50 percent, and after a few trials and errors, the first piece designed as a panhandle was produced with a few minor errors after 10 hours of printing. Those minor errors were later fixed manually.

Figure 9.1: Modified panhandle

The second part that was pressed was the rocker of the mechanism, and this link is the main arm that carries the pan. Since this mechanism was designed symmetrically, we had to print two of some parts. This piece was one of the pieces that we had to print two. The printing process took 8 hours per piece.

Figure 9.2: Rocker of the mechanism.

After the long pieces were produced, the first piece printed was the short arm of the mechanism. In the symmetrical version of this part, they were not completely symmetrical as there was a shaft hole of the motor, or to crank mechanism. After an entire printing process of 6 hours, these two pieces were in our hands.

Figure 9.3: Crank links of the mechanism.

In order for the printed parts to be joined to each other, we first had to put bearings in their bearing holes. Except for the first printed part, the bearings of the other parts were put into place without much trouble. When placing the bearing on the first part, the bearings did not fit properly due to an error that we thought was caused by the manual processing of the part. During the installation of the bearings, our first part cracked and considerably reduced the part's durability. We solved this problem by partially melting part of the piece and pouring glue into the cracks.

Figure 9.4: Ground structure of the mechanism.

Figure 9.5: Working prototype of the mechanism.

10 Discussions and Conclusion

One DoF frying pan shaker mechanism were constructed for automating shaking process in this study. Essential feature of this mechanism is it's degrees of freedom. Since mechanism is one DoF, we can control all the process by on single DC motor. This just don't eliminate the need of control but also reduces overall electrical cost.

Pan shaking motion were captured by filming the motion and analysed the motion by Tracker software. Body guidance synthesis procedure were fed with 4 precision points which we gathered from *tracker* software. Then this results are adjusted so that cost of manufacturing can be reduced and fit the printing space we had in our hand. In summary, a new handle for the pan, 4 links and 2 ground are designed and produced to realise this mechanism.

Since DC motors were a little bit exceed our budget, a crank lever is designed and produced to rotate the crank link. This lever then link then connected to the crank of the mechanism and motion is supplied with human power.

Main problem that is encountered when designing the mechanism was long printing processes. The problems couldn't be anticipated become very hard to fix since we couldn't just print a better version all over again. So some of the links were modified with heated skewer.

Bearings were really tight fits so the bearing slots had to be sanded a little bit to avoid cracking.

Lastly the mechanism had to fixed to the ground via a heavy block in order to avoid shaking but heavy blocks aren't cheap and since we exceed our budged already we just used a relatively heavy wood piece.

References

[1] Erkin Gezgin, Pyung Chang, and Ahmet Akhan. "Synthesis of a Watt II six-bar linkage in the design of a hand rehabilitation robot". In: *Mechanism and Machine Theory* 104 (Oct. 2016), pp. 177–189. DOI: 10.1016/j.mechmachtheory.2016.05.023.

[2] Mark Plecnik, J. Michael McCarthy, and Charles W. Wampler. "Kinematic Synthesis of a Watt I Six-Bar Linkage for Body Guidance". In: *Advances in Robot Kinematics*. Ed. by Jadran Lenarčič and Oussama Khatib. Cham: Springer International Publishing, 2014, pp. 317–325. ISBN: 978-3-319-06698-1. DOI: 10.1007/978-3-319-06698-1_33. URL: https://doi.org/10.1007/978-3-319-06698-1_33.